Why spontaneous symmetry breaking disappears in a bridge system with PDE-friendly boundaries

Vladislav Popkov* and Gunter M. Schütz

Institut für Festkörperforschung, Forschungszentrum Jülich, D-52425 Jülich, Germany

(Dated: 2nd February 2008)

Abstract

We consider a driven diffusive system with two types of particles, A and B, coupled at the ends to reservoirs with fixed particle densities. To define stochastic dynamics that correspond to boundary reservoirs we introduce projection measures. The stationary state is shown to be approached dynamically through an infinite reflection of shocks from the boundaries. We argue that spontaneous symmetry breaking observed in similar systems is due to placing effective impurities at the boundaries and therefore does not occur in our system. Monte-Carlo simulations confirm our results.

*Present address : Institut für Theoretische Physik, Universität zu Köln, Zülpicher Str. 77, D-50937 Cologne, Germany

I. INTRODUCTION

Systems of driven diffusing particles attract attention because, despite their relative simplicity, they embrace a whole range of critical phenomena far from thermal equilibrium [1–3]. One of the remarkable features is the appearance of phase transitions induced by spatial boundaries of a system, studied in detail for models with one species of particles [4–8] and for some multi-species models [9–12]. The ability of a nonequilibrium system to "feel" the boundaries constitutes a key feature of driven systems: in fact, the boundaries dominate the bulk giving rise to the phase transitions. Therefore it is clear that boundary conditions play a crucial role and have to be chosen with care, strictly adequate to the physical situation which is being modelled. To this end one has to define specific boundary rates for injection and extraction of particles at the ends of the system. There are several possible strategies.

One of them is to postulate the most simple boundary rates, and treat the rates themselves as parameters. A system is studied, then, as a function of those parameters, so that one tries to keep their number small. This approach is used, e.g., in [4, 9].

Another approach, let us call it *particle boundary reservoir approach*, treats the boundary problem of a driven diffusive system as if it was coupled at the ends to reservoirs of particles with fixed particle densities. In this case, the rates are *dictated* by the reservoir particle densities and by themselves do not, in general, look simple. The boundary rates are fixed such that the stationary measure of the process with equal reservoir densities on the left and on the right is essentially equal to the stationary measure of the infinite system with the same particle densities, see below for a detailed discussion. Thus reservoir particle densities are parameters, namely, reservoir densities of each species of particles at each boundary. Correspondingly, in the one-dimensional case, where there are two (left and right) boundaries, the number of parameters is equal to $2 * number\ of\ species$ in the system. This approach is used in [8, 10, 13]. We argue that in this case there exists a well-defined hydrodynamic limit, and the original stochastic problem has correspondingly a well-behaved coarse-grained description via conservation law equations. The latter constitutes a powerful tool to study the physics of the system, e.g., phase diagrams and the location and type of phase transitions.

In some important cases the two approaches are equivalent. For instance, for the ASEP

with open boundaries, the rates of injection α and extraction β respectively are expressed as $\alpha = \rho_L, \beta = 1-\rho_R$ in terms of the particle boundary reservoir approach. In more complicated settings one may attribute effective boundary densities to given boundary rates. In this way a very large class of single-species systems with open boundaries can be described and their phase diagram can be predicted in terms of the boundary densities [8]. For attractive single-species systems the validity of this approach has been proved rigorously in very recent work [14]. The purpose of this paper is to demonstrate that in two-species models, however, the two approaches cannot generally be substituted with one another. We exhibit this difference and discuss its significance for the appearance of spontaneous symmetry breaking in an ABO model [9], which is a paradigmatic two-species model [15].

To this end, we first introduce the model (Sec. II), discuss its hydrodynamic properties under Eulerian scaling (Sec. III) and show how to construct appropriate boundary reservoirs (Sec. IV). The strategy employed here can be applied to any stochastic particle system. Then we show (Sec. V) that the phenomenon of infinite reflections of shock fronts from the boundaries [16] exists also in the ABO system which is much studied, and is known to have many intriguing features. Using this we arrive at the conclusion (Sec. VI) that the so-called bridge model [9] (which is an ABO model with specific injection and extraction rates) has spontaneous symmetry breaking due to the fact that the boundary injection and extraction rates place effective obstacles at the ends of the chain, rather than corresponding to boundary reservoirs with some effective boundary density. We demonstrate that with these effective obstacles removed, there is no symmetry breaking phase transition. Thus, symmetry breaking can be viewed as an impurity-induced effect. Moreover, we argue that the original bridge model may have symmetry breaking transition precisely at the point where a hydrodynamic description with effective boundary densities breaks down. We summarize our main conclusion in the final Sec. VII.

II. THE MODEL

The ABO model is defined on a chain of length N. There are particles of type A and of type B, distributed along the chain. Any site of the chain can be empty, or contain at most one particle. In the bulk, exchange with the nearest neighbours happens, e.g., a particle A can exchange with a hole 0 on its right $A0 \Rightarrow 0A$ with rate Γ_{A0}, etc.. The complete set of

rates is given as follows

$$\begin{aligned} A0 &\Rightarrow 0A \qquad \text{with rate } \Gamma_{A0} \\ 0A &\Rightarrow A0 \qquad \text{with rate } \Gamma_{0A} \\ B0 &\Rightarrow 0B \qquad \text{with rate } \Gamma_{B0} \\ 0B &\Rightarrow B0 \qquad \text{with rate } \Gamma_{0B} \\ AB &\Rightarrow BA \qquad \text{with rate } \Gamma_{AB} \\ BA &\Rightarrow AB \qquad \text{with rate } \Gamma_{BA} \end{aligned} \tag{1}$$

The boundary conditions correspond to reservoirs of particles with fixed densities ρ_L^A, ρ_L^B and ρ_R^A, ρ_R^B at the left and at the right end of the chain respectively and are defined in the section IV. For a specific choice of rates [17],

$$\Gamma_{AB} - \Gamma_{BA} = (\Gamma_{A0} - \Gamma_{0A}) + (\Gamma_{0B} - \Gamma_{B0}), \tag{2}$$

the stationary state on a ring is given by a product measure, which does not crucially affect the qualitative properties of the system, but significantly reduces computational difficulties (since no approximation in the calculation of the bulk flux, boundary conditions are required). We shall follow this choice below, making comments on the general situation when necessary. In most cases, we shall take

$$\Gamma_{A0} = \Gamma_{0B} = \Gamma_{AB}/2 = 1, \quad \Gamma_{0A} = \Gamma_{B0} = \Gamma_{BA} = 0 \tag{3}$$

without losing generality.

III. HYDRODYNAMIC LIMIT EQUATIONS

Here we shall treat for simplicity the case (3) where there is a product measure state on a ring. From this property and the hopping rules (3) exact stationary fluxes are given by

$$j^A(\rho^A, \rho^B) = \rho^A(1 - \rho^A + \rho^B) \tag{4}$$

$$j^B(\rho^A, \rho^B) = -\rho^B(1 - \rho^B + \rho^A). \tag{5}$$

Following [18], the hydrodynamic equations of our process may be obtained by averaging, factorizing and Taylor expanding the lattice equations of motion with respect to the lattice

constant $a \ll 1$. In the first order of the expansion, one obtains

$$\begin{aligned}
\frac{\partial \rho^{\mathrm{A}}}{\partial t'} + \frac{\partial j^{\mathrm{A}}(\rho^{\mathrm{A}}, \rho^{\mathrm{B}})}{\partial x} &= \varepsilon \frac{\partial}{\partial x}\left(\frac{\partial \rho^{\mathrm{A}}}{\partial x} + \left(\frac{\partial \rho^{\mathrm{A}}}{\partial x}\rho^{\mathrm{B}} - \frac{\partial \rho^{\mathrm{B}}}{\partial x}\rho^{\mathrm{A}}\right)\right) \\
\frac{\partial \rho^{\mathrm{B}}}{\partial t'} + \frac{\partial j^{\mathrm{B}}(\rho^{\mathrm{A}}, \rho^{\mathrm{B}})}{\partial x} &= \varepsilon \frac{\partial}{\partial x}\left(\frac{\partial \rho^{\mathrm{B}}}{\partial x} + \left(\frac{\partial \rho^{\mathrm{B}}}{\partial x}\rho^{\mathrm{A}} - \frac{\partial \rho^{\mathrm{A}}}{\partial x}\rho^{\mathrm{B}}\right)\right) \\
\varepsilon = \frac{a}{2} \to 0; \;\; \frac{\partial}{\partial t} &= 2\varepsilon \frac{\partial}{\partial t'}
\end{aligned} \tag{6}$$

For a finite system with open boundaries this is supplemented with the boundary conditions

$$\rho^{\mathrm{Z}}(0,t) = \rho_L^{\mathrm{Z}}, \quad \rho^{\mathrm{Z}}(N,t) = \rho_R^{\mathrm{Z}} \,, \qquad Z = A, B \tag{7}$$

The system of equations (6), after the substitutions $\rho = 1 - \rho^A - \rho^B, u = \rho^B - \rho^A$, becomes

$$\begin{aligned}
\frac{\partial \rho}{\partial t} + \frac{\partial}{\partial x}(\rho u) &= \varepsilon \frac{\partial^2 \rho}{\partial x^2} \\
\frac{\partial u}{\partial t} + \frac{\partial}{\partial x}\left(\rho + u^2\right) &= \varepsilon \frac{\partial}{\partial x}\left(\frac{\partial u}{\partial x} + \left(u\frac{\partial \rho}{\partial x} - \rho \frac{\partial u}{\partial x}\right)\right),
\end{aligned} \tag{8}$$

which in its inviscid form ($\varepsilon = 0$) has been derived rigorously for our model defined on the infinite lattice [19] and is known in the theory of conservation law equations as the Leroux´s equation. It appears in many applications, further details about this equation can be found in [19, 20]. Note that the viscosity term is required for uniqueness of the solution of the hydrodynamic equation. For an infinite system the choice of viscosity has some arbitraryness. However, in the presence of the boundaries the exact form of the viscosity matrix becomes important in systems with more than one conservation law [21]. The question how the macroscopic boundary condition (7) on the PDE can be realized on microscopic lattice gas scale is addressed in the following sections.

IV. BOUNDARY RESERVOIRS AND PROJECTION MEASURES

In driven (nonequilibrium) systems, the steady state is governed not only by local interactions in the bulk, but also by interaction with boundaries. To define a boundary reservoir, we introduce a projection measure for a subsystem of a larger system (defined on a spatial domain Ω) by defining the following marginal: a measure is a *projection measure* for a spatial domain $Q \subseteq \Omega$ if *all its correlations* are identical to those of the whole system Ω inside the domain Q.

In what follows we consider as domain Q a finite system of N sites as a subsystem of an infinite system where Ω is the integer lattice Z. For illustration we first consider $N = \infty$ (semi-infinite system with a left boundary). In the case of a product measure, the projection measure is especially simple: it remains a product measure for all sites in Q, i.e., homogeneous initial distribution with an average densities $\rho^A_{\rm bulk}, \rho^B_{\rm bulk}$ of A and B particles. In vector notation [1] the projection measure for the semi-infinite system is given by

$$|P(0)\rangle = \prod_{k=1}^{\infty} \otimes \begin{pmatrix} \rho^A_{\rm bulk} \\ \rho^B_{\rm bulk} \\ 1 - \rho^B_{\rm bulk} - \rho^A_{\rm bulk} \end{pmatrix}. \tag{9}$$

Similarly, for a finite subsystem of the length N one has the projection measure

$$|P\rangle = \prod_{i=1}^{N} \otimes \begin{pmatrix} u \\ v \\ 1 - u - v \end{pmatrix}, \tag{10}$$

where $u = \rho^A_{\rm bulk}, v = \rho^B_{\rm bulk}$.

So far we have discussed only measures. To make the connection to stochastic dynamics we assume that the particle system defined on the infinite lattice has a product measure as its steady state. In order to define dynamics for an open system with creation and annihilation of particles corresponding to a boundary reservoir with densities $\rho^A_L = u, \rho^B_L = v$ for a semi-infinite system, we demand that the projection measure (9) stays invariant for $u = \rho^A_{\rm bulk}, v = \rho^B_{\rm bulk}$. This is a natural requirement, since one has a perfect match of the product state with the boundaries. In the same way, we can define the right boundary reservoir for a semi-infinite chain $k = -\infty, 0$, and for a finite chain of the length N, with the projection measure (10), where $\rho^A_L = \rho^A_R = u$, $\rho^B_L = \rho^B_R = v$. Some examples illustrating more general situations (e.g., involving an Ising measure) can be found in [8, 10, 13].

In general, there are many ways to obtain boundary rates which leave the projection measure invariant. In order to calculate boundary rates for our model we first require that particles are injected only at the edges (sites $1, N$) of the lattice, corresponding to the nearest neighbor hopping in the bulk of the chain. Furthermore we note that, in particular, one requires the stationary flux in the system with equal reservoir densities $\rho^A_L = \rho^A_R = u$, $\rho^B_L = \rho^B_R = v$ to be equal to the stationary flux in an infinite system with the densities u, v.

The stationary flux is

$$j^A(u,v) = u(1-u+v) \tag{11}$$

$$j^B(u,v) = -v(1-v+u). \tag{12}$$

The different signs of j^A and j^B are due to the fact that A-particles and B-particles hop in opposite directions. On the other hand, the stationary flux of particles A through the left boundary is

$$j_L^A = \langle 0\rangle \Gamma_{A0}^L + \langle B\rangle \Gamma_{AB}^L \tag{13}$$

where Γ_{XY}^L is the rate of exchange of particle of the sort X (from the left reservoir) with the particle of sort Y at the first site and $\langle Y\rangle$ is the stationary expectation value to find a particle Y at the first site. In the stationary state, the latter is equal to the density (see (10)): $\langle B\rangle = v,\ \langle 0\rangle = 1-u-v$. Inserting these expressions in (13), we get

$$j_L^A = (1-u-v)\Gamma_{A0}^L + v\Gamma_{AB}^L$$

Repeating the arguments for the flux of particles B through the left boundary, we obtain

$$j_L^B = -\langle B\rangle \Gamma_{0B}^L - \langle B\rangle \Gamma_{AB}^L = -v(\Gamma_{0B}^L + \Gamma_{AB}^L)$$

We require the above expressions to be equal to the stationary fluxes (11),(12).This leaves one parameter undefined, since there are 3 unknown boundary rates Γ and two relations. To get an additional relation, consider another correlation, e.g. the probability to find particles A, B on the first two sites, $\langle AB\rangle$. The time evolution of this correlation is

$$\frac{\partial}{\partial t}\langle AB\rangle = \Gamma_{A0}^L\langle 0B\rangle + \Gamma_{0B}\langle A0B\rangle + \Gamma_{AB}\langle AAB\rangle - \Gamma_{AB}\langle AB\rangle.$$

In the stationary state, left hand side vanishes, and the correlations are given by (10) $\langle 0B\rangle = (1-u-v)v$, $\langle AB\rangle = uv$, $\langle AAB\rangle = u^2v$, $\langle A0B\rangle = u(1-u-v)v$. Substituting the bulk rates Γ_{XY} from (3), we get $\Gamma_{A0}^L = u$, which, together with the relations $j_L^A = j^A$, $j_L^B = j^B$ fixes all boundary rates to be

$$\Gamma_{A0}^L(u,v) = u; \quad \Gamma_{AB}^L(u,v) = 2u; \quad \Gamma_{0B}^L(u,v) = (1-u-v). \tag{14}$$

It is interesting to note that the rates (14) can be obtained from another simple argument. In a boundary reservoir with the densities $\rho_L^A = u$, $\rho_L^B = v$, the probability to find a particle

A, B and a hole 0 is $p(A) = u$, $p(B) = v$, $p(0) = 1 - u - v$. We assume the rates of hopping of the particles from the reservoir to the site 1 of the system to be given by the bulk rates (3) multiplied by corresponding probabilities, i.e.,

$$\Gamma^L_{A0} = p(A)\Gamma_{A0}, \;\; \Gamma^L_{0B} = p(0)\Gamma_{0B}, \quad \Gamma^L_{AB} = p(A)\Gamma_{AB}. \tag{15}$$

This yields (14).

Analogously, on the right boundary, the rates Γ^R_{XY} of exchange of particle X at site N with the particle Y (from the right reservoir) is

$$\Gamma^R_{A0} = p(0)\Gamma_{A0}, \;\; \Gamma^R_{0B} = p(B)\Gamma_{0B}, \quad \Gamma^R_{AB} = p(B)\Gamma_{AB} \tag{16}$$

or

$$\Gamma^R_{A0}(u,v) = (1-u-v), \quad \Gamma^R_{0B}(u,v) = v, \quad \Gamma^R_{AB}(u,v) = 2v. \tag{17}$$

One verifies straightforwardly that for the choice of the rates (14), (17) the projection measure (10) is stationary.

For the boundary reservoirs with arbitrary densities ρ^A_R, ρ^B_R on the right and ρ^A_L, ρ^B_L on the left we shall use the boundary rates given by $\Gamma^R_{XY}(\rho^A_R, \rho^B_R)$ and $\Gamma^L_{XY}(\rho^A_L, \rho^B_L)$ respectively. We shall call such boundary rates PDE-friendly, since, as we show in the next section, they allow for an adequate hydrodynamic description for a finite open system.

V. INFINITE REFLECTIONS OF SHOCK FRONTS FROM THE BOUNDARIES. ABSENCE OF SPONTANEOUS SYMMETRY BREAKING.

It is an open problem how to obtain a hydrodynamic description of a two species system with open boundaries. A step towards such a description has been made in [16]. It has been demonstrated that the evolution to the stationary state can proceed through an infinite sequence of reflections of a domain wall with the boundaries of the system. It is interesting to study the reflections for the system (3) to see if it provides another example where this scenario applies. Note that the model we investigate here and the one investigated in [16] have topological differences: in the latter, particle dynamics on two parallel chains was considered, and particles on both chains hopped in the same direction. Instead, in the presently considered model (3), particles occupy one chain and hop in opposite directions.

A. Reflection maps

To pose a reflection problem, take a half-infinite chain with only one, e.g., left boundary, corresponding to left boundary reservoir densities $\rho_L^A = u, \rho_L^B = v$, and choose an *initial state* to be a projection measure of a stationary state for an infinite system onto the positive half-infinite chain (9), i.e., homogeneous initial distribution with an average densities $\rho^A_{\rm bulk}, \rho^B_{\rm bulk}$ of A and B particles. We consider bulk rates (3) and corresponding boundary rates (14).

If the bulk densities coincide with the left boundary densities $\rho^A_{\rm bulk} = u, \rho^B_{\rm bulk} = v$, the initial distribution (9) stays invariant because of the perfect match of the initial state with the boundaries. Otherwise, there is a mismatch at the boundary which has to be resolved. In this case, Monte Carlo simulations lead to one of the following scenarios: (a) a thin boundary layer develops interpolating between the bulk densities $\rho^{A,B}_{\rm bulk}$ and boundary densities u, v, and stays always attached to the left boundary, (b) a shock wave of the densities r^A, r^B develops and propagates to the right, (c) a rarefaction wave with the density r^A, r^B forms and spreads to the right. The scenario (b) is demonstrated on Fig.1, showing Monte-Carlo evolution of a state (9) with $\rho^{A,B}_{\rm bulk} = (0.1, 0.7),\ \ u, v = 0.25, 0.55$ after $t = 300$ Monte Carlo steps. Like in [16], we mimic the half-infinite chain with a finite chain with the right boundary conditions matching perfectly the bulk densities. As a result, after time t the density profile, while staying unchanged on the right boundary (see Fig.1), at the left boundary develops the shock with the densities $r^A \approx 0.348, r^B \approx 0.131$ spreading to the right. Due to particle number conservation in the bulk, a Z-component of the shock interface moves with the velocity

$$V^Z = \frac{j^Z_{\rm bulk} - j^Z_{\rm r}}{\rho^Z_{\rm bulk} - r^Z}\ , \tag{18}$$

where we used the short notations $j^Z_{\rm bulk} = j^Z(\rho^A_{\rm bulk}, \rho^B_{\rm bulk})$, $j^Z_{\rm r} = j^Z(r^A, r^B)$. Since there is an interaction between A and B species, the velocities must coincide in both components: $V^A = V^B$, or

$$\frac{j^A_{\rm bulk} - j^A_{\rm r}}{\rho^A_{\rm bulk} - r^A} = \frac{j^B_{\rm bulk} - j^B_{\rm r}}{\rho^B_{\rm bulk} - r^B}, \tag{19}$$

defining implicitly the allowed location of the points r^A, r^B. In our case, the above relation becomes (see 4,5):

$$\frac{\rho^A_{\rm bulk}(1 - \rho^A_{\rm bulk} + \rho^B_{\rm bulk}) - r^A(1 - r^A + r^B)}{\rho^A_{\rm bulk} - r^A} = \frac{-\rho^B_{\rm bulk}(1 - \rho^B_{\rm bulk} + \rho^A_{\rm bulk}) + r^B(1 - r^B + r^A)}{\rho^B_{\rm bulk} - r^B} \tag{20}$$

Here we implicitly assume the fluxes of the reflected wave to be given by stationary fluxes with the densities r^A, r^B. This supposition is justified because for random initial conditions used here the system away from the shock is locally stationary.

Analogously one can consider the right boundary reflection, taking a half-infinite chain with right boundary only and initial product measure state (9) where the product goes from $-\infty$ to L. An example of a right boundary reflection is shown on Fig.2. Again, the shock wave resolving the mismatch at the boundary appears and spreads to the left. For the same reasons as were given above for left boundary reflection, the densities of reflected waves r^A, r^B satisfy relation (20). Solutions of (20) are two families of straight lines

$$r^B - \rho^B_{\rm bulk} = (r^A - \rho^A_{\rm bulk})\gamma_+(\rho^A_{\rm bulk}, \rho^B_{\rm bulk}), \qquad \gamma_+(s,t) = \frac{1}{2s}\left(-2+s+t+\sqrt{(s+t-2)^2-4st}\right). \tag{21}$$

$$r^B - \rho^B_{\rm bulk} = (r^A - \rho^A_{\rm bulk})\gamma_-(\rho^A_{\rm bulk}, \rho^B_{\rm bulk}), \qquad \gamma_-(s,t) = \frac{1}{2s}\left(-2+s+t-\sqrt{(s+t-2)^2-4st}\right). \tag{22}$$

The solutions with bigger γ corresponds to the left reflection, and another to the right reflection. Note that $\gamma_\pm(s,t)$ are real in the physical domain $0 \le s+t \le 1$. The meaning of the above equations is twofold. One of them was given above, that is, for any given $\rho^A_{\rm bulk}, \rho^B_{\rm bulk}$, the reflected waves must have densities satisfying (21),(22). Another, alternative, is: given the reflected wave densities r^B and r^A, the initial bulk densities (which have led to those reflected waves), must satisfy the equation equivalent to (21,22).

$$\rho^B_{\rm bulk} - r^B = (\rho^A_{\rm bulk} - r^A)\gamma_\pm(r^A, r^B), \tag{23}$$

where $\gamma_\pm(s,t)$ are defined in (21,22). The equation above is a solution of (20), because the latter is completely symmetric with respect to the exchange $r^Z \leftrightarrow \rho^Z_{\rm bulk}$. On the basis of Monte-Carlo calculations and investigation of the hydrodynamic limit equations the following observation can be made:

The collection of all possible densities r^A, r^B of the waves, resulting from the left boundary reflection (with boundary densities u, v) with whatever initial conditions $\rho^A_{\rm bulk}, \rho^B_{\rm bulk}$, constitute some curve $\mathcal{L}(u,v)$, completely parametrized by this point u, v, and containing this point. All initial bulk densities satisfying (23) for certain point r^A, r^B of $\mathcal{L}$, result in the reflected wave with the densities r^A, r^B. The same is true for right boundary reflection, with the curve $\mathcal{L}$ replaced by $\mathcal{R}$.

The mapping from arbitrary $\rho^A_{\rm bulk}, \rho^B_{\rm bulk}$ to resulting r^A, r^B is described by means of reflection maps introduced in [16]. Typical examples of left and right reflection maps are shown on Figs. 4 and 3.

Each of the reflection maps of the type shown in Figs. 3 and 4 is parametrized by a single point u, v (which has a meaning of the left/right boundary density for left/right map). Each point $0 \leq u + v \leq 1$ corresponds to a different map. Classification of all different maps requires separate investigation. Here we shall find out what happens if we fix the right and the left boundary corresponding to the reflection maps Fig. 4 and Fig. 3. Let us take an initial homogeneous state with the densities, fitting the density of the left reservoir, $\rho^A_{\rm bulk}, \rho^B_{\rm bulk} = \rho^A_L, \rho^B_L$. As the result of the first interaction with the right boundary, a reflected wave forms, with the densities r^A_0, r^B_0 given by the intersection of the line (22) with the curve $\mathcal{R}$ of Fig. 4. This reflected wave hits the left boundary then, resulting in the next reflected wave with the densities r^A_1 ,r^B_1. The left reflection is controlled by the curve $\mathcal{L}$ at Fig. 3, therefore the densities of the reflected wave r^A_1, r^B_1 are given by the intersection of the line (21), where new $\rho^A_{\rm bulk}, \rho^B_{\rm bulk} = r^A_0$, r^B_0, with the curve $\mathcal{L}$. Since the curves $\mathcal{R}$,$\mathcal{L}$ do not coincide with any of the lines defined by (14), (17), this process continues forever, though converging to the stationary state $\mathcal{S}$, the point of the intersection of $\mathcal{L}$ with $\mathcal{R}$, see Fig. 5. After $2k-1$ reflections, the wave with the densities r^A_{2k-1}, r^B_{2k-1} will hit the right boundary, producing the reflected wave of the densities r^A_{2k}, r^B_{2k}, corresponding to the intersection of the line (22) (with $\rho^A_{\rm bulk}, \rho^B_{\rm bulk} = r^A_{2k-1}$, r^B_{2k-1}) with the curve $\mathcal{R}$. The latter wave, hitting the left boundary, produces the next reflected wave, and so on. This process is depicted schematically on Fig. 6. Several remarks are in order.

- The densities $\{r^A_k,\, r^B_k\}_{k=0}^{\infty}$ of the reflected waves constitute a converging sequence. Convergence is exponential, $\delta u_{n+2k} = e^{-\kappa k}\delta u_n$, for $n \to \infty$ where we denote by δu_n the deviation from the stationary density at the n-th step. $e^{-\kappa} < 1$ is a constant depending on tangential derivatives $\alpha, \beta, \alpha_1, \beta_1$ of the curves $\mathcal{R}$,$\mathcal{L}$ and the characteristic curves(14), (17), respectively, at the stationary point $\mathcal{S}$, $e^{-\kappa} = (1 - \frac{tg(\alpha_1)}{tg(\alpha)})(1 - \frac{tg(\beta_1)}{tg(\beta)})/((1 + \frac{tg(\alpha_1)}{tg(\beta)})(1 - \frac{tg(\beta_1)}{tg(\alpha)}))$. Note that if at least one of the characteristic derivatives happens to coincide with $\alpha_1, \beta_1 (\alpha = \alpha_1$ or $\beta = \beta_1)$ then the sequence converges in one step.

- The velocities of reflected waves for large k converge to the finite characteristic ve-

locities computed at the stationary point $\mathcal{S}$, as eigenvalues of the flux Jacobian, see [18].

- The stationary densities are not reached at any finite time. Strictly speaking, the stationary density is reached exponentially in time with characteristic time proportional to the length of the system N. On the contrary, in one-species models like the ASEP, the corresponding characteristic time is of order of 1/(rate of hopping).

We conclude that for the system (3) with PDE-friendly boundary rates $\Gamma^L_{XY}(\rho^A_L, \rho^B_L), \Gamma^R_{XY}(\rho^A_R, \rho^B_R)$, given by (14), (17), the convergence to a stationary state through an infinite number of reflections is a generic feature of the dynamics. This is confirmed by the good agreement of the Monte-Carlo simulation of the lattice model with the numerical integration of hydrodynamic PDE's (6), see Figs.1, 2, 5, 7. Without the PDE-friendly boundary rates already the result of the first reflection would be unpredictable.

B. Symmetric boundary conditions

In the preceeding subsection we gave an example for the time evolution of the system in case of generic boundary conditions. Here we consider a situation when the boundary rates possess the symmetry with respect to a simultaneous right-left reflection and an exchange of A particles with B particles, i.e., the same symmetry as in the similar models where spontaneous symmetry breaking has been observed [9, 22]. This amounts to the following restriction of the boundary reservoir densities:

$$\rho^A_R = \rho^B_L, \quad \rho^B_R = \rho^A_L. \tag{24}$$

Analysis of reflection maps for our PDE-friendly boundary rates (14,17) allows us to conclude, that there is no spontaneous symmetry breaking — the stationary state is always symmetric (i.e., corresponds to equal densities of A- and B-particles). A typical reflection map for the case (24) is presented in Fig.7. The reason why there is spontaneous symmetry breaking in the bridge model [9] will be given in the next section.

VI. WHY THE HYDRODYNAMIC LIMIT FAILS FOR THE BRIDGE MODEL

The bridge model is defined on a finite chain of the length N, where the processes in the bulk with rates

$$\Gamma_{A0} = \Gamma_{0B} = 1, \Gamma_{AB} = q, \quad \Gamma_{0A} = \Gamma_{B0} = \Gamma_{BA} = 0 \tag{25}$$

are complemented with the processes at the boundaries. On the left boundary site

$$\Gamma^L_{A0} = \alpha = \alpha\Gamma_{A0}, \;\; \Gamma^L_{0B} = \beta = \beta\Gamma_{0B}, \quad \Gamma^L_{AB} = 0 \tag{26}$$

and on the right boundary site,

$$\Gamma^R_{0B} = \alpha = \alpha\Gamma_{0B}, \;\; \Gamma^R_{A0} = \beta = \beta\Gamma_{A0}, \quad \Gamma^R_{AB} = 0. \tag{27}$$

The model is invariant with respect to simultaneous left-right and A -B interchange. Nevertheless, for certain range of parameters, typically for large α and small β, the state of the system is characterized by a phase where the average densities of particles are not symmetric: the symmetry between A and B is broken spontaneously, and it takes a system a very long time (which grows exponentially with the system size) to get from the state with a prevalence of A-particles to the state with a prevalence of B-particles. The exchange rate q is not crucial for the occurence of this intriguing phenomenon.

(a) Let us consider $q = 2$ and try to see if one can associate a reservoir density as described above to the rates (26), (27). In terms of the probabilities $p(A), p(B), p(0)$ to find a particle of sort A, B and 0 respectively in the reservoir, the left reservoir rates are given in (15). Comparing (26) with (15), we obtain relations

$$p(A) = \alpha, p(0) = \beta, p(A) = 0,$$

incompatible between themselves.

(b) Let us nevertheless try to find *effective* boundary densities for the rates (26, 27) for general q. It is instructive to analyze the case when both injection and extraction are small $\alpha, \beta \ll 1$ and $\alpha < \beta$. Then, the typical time to inject a particle is bigger than the typical time to extract a particle $\tau_{in} = \alpha^{-1} > \beta^{-1} = \tau_{out}$, and both $\tau_{in}, \tau_{out} \gg 1$. In this case, one can associate boundary densities as it is done in the usual asymmetric exclusion process (ASEP): $\rho^A_L = \alpha, \rho^B_L = 1 - \beta$, and $\rho^A_R = 1 - \beta, \rho^B_R = \alpha$. Correspondingly, the density of holes in the boundary reservoirs is $1 - \rho^A - \rho^B$, yielding

$$\rho^0_R = \rho^0_L = \beta - \alpha. \tag{28}$$

We see that for $\alpha > \beta$ the density of holes (28) becomes *negative*, which signals a breakdown of the reservoir picture across the point $\alpha = \beta$ when $\alpha, \beta \ll 1$. And this point lies exactly at the phase transition line to the symmetry broken phase [22]. Thus, we have shown that for parameters where symmetry breaking phase is observed, the hydrodynamic description, using boundary reservoirs, fails. A natural interpretation of the rates (26), (27) would be that they effectively correspond to impurities, placed at the left and at the right boundary of the system, and preventing $A - B$ exchange. It is solely due to these obstacles, that spontaneous symmetry breaking actually happens. An effective hydrodynamic description may still be valid in the symmetric phase.

The above considerations are valid for (a) $q = 2$, α, β arbitrary and (b) q arbitrary and α, β small. However, we believe that a similar description is valid for any q, α, β. Since for $q = 2$ as well as for $q = 1$ there are no correlations between particles and vacancies, a perfect hydrodynamic description of the bridge model will be achieved according to the result of the previous section, if exchange at the boundaries between A, B happens *on the same footing as in the bulk*, see the discussion below (14), which amounts to choosing

$$\Gamma^L_{AB} = \Gamma^R_{AB} = q\alpha, \qquad q = 1, 2 \tag{29}$$

in (26), (27). For the above choice, a hydrodynamic description with fixed boundary densities is valid for all α, β leading to the complete disappearance of the symmetry broken phase from the phase diagram. For instance, for $q = 1$, the A-particle cannot distiguish between B-particle and a hole, both in the bulk and in the boundaries (and the same is valid for B-particles), so that the system effectively separates into two one-species problem ASEP, with injection rate α and extraction rate $\alpha + \beta$. Invoking the known solution for ASEP phase diagram [5],[6], we find that the exact stationary state density of a PDE-friendly bridge model with $q = 1$ is

$$\rho^A_{stat} = \rho^B_{stat} = \alpha, \ \text{ if } \alpha < \frac{1}{2}$$
$$\rho^A_{stat} = \rho^B_{stat} = \frac{1}{2}, \ \text{ if } \alpha \geq \frac{1}{2}.$$

Note also that the stationary state in this case, as opposed to the $q = 2$ case considered earlier, is reached after *single* interaction of a shock wave, or a rarefaction wave, with the boundary, like in the ASEP [16].

VII. CONCLUSIONS

We have investigated the ABO model and, defining projection measures, introduced boundary conditions compatible with a hydrodynamic description. We have studied the system for boundary rates which are either symmetric or nonsymmetric with respect to left-right reflection and exchange of particle species. Investigating the reflection of shocks at the boundaries, we conclude that the system with symmetric PDE-friendly boundary conditions has a stationary symmetric phase in all parameter space. The relaxation to the stationary state proceeds by an infinite sequence of reflections with the boundaries, which can be described using reflection maps. Hydrodynamic limit equations are constructed and studied, yielding results consistent with the stochastic dynamics. For the bridge model, which is a special case of the ABO model, we showed that at the phase transition to the spontaneously broken phase the hydrodynamic description fails. While our discussion was in the framework of the ABO model, we believe that similar results are valid for other driven diffusive systems with two conservation laws, such as two-lane models [10, 18, 23, 24] or bricklayer models with nonconserved internal degrees of freedom [25].

We conclude that any choice of boundary rates which does not correspond to certain densities of boundary reservoirs is equivalent to placing an impurity at the respective boundaries. This entails extra complexity and rate-dependent nonuniversal behaviour. Sometimes the impurity thus introduced leads only to a local disturbance and correspondingly to a redefinition of boundary densities. In other cases, however, the impurity effect is highly nonlocal and nontrivial. This last case is very pronounced in the case of spontaneous symmetry breaking considered in [9]. It would be interesting to see if for any other choice of the $A-B$ boundary exchange rates $0 \leq \Gamma_{AB}^{L} = \Gamma_{AB}^{R} < q\alpha$ there will be a region in the phase space α, β (shrinking as $\Gamma_{AB}^{L}, \Gamma_{AB}^{R}$ increase) where the symmetry broken phase will exist.

Acknowledgments

We thank D. Mukamel, R. Willmann and C. Bahadoran for fruitful discussions. V.P. thanks Deutsche Forschungsgemeinschaft for financial support.

---

[1] G. M. Schütz, *Exactly solvable models for many-body systems far from equilibrium* (Academic Press, London, 2000), in: Phase Transitions and Critical Phenomena, ed. C.Domb and J.L. Lebowitz, Vol. 19.

[2] T. M. Liggett, *Stochastic interacting systems: contact, voter and exclusion processes* (Springer, Berlin, 1999).

[3] B. Schmittmann and R. K. P. Zia, *Statistical Mechanics of Driven Diffusive Systems* (Academic Press, London, 1995), in: Phase Transitions and Critical Phenomena, ed. C.Domb and J.L. Lebowitz, Vol. 17.

[4] J. Krug, Phys. Rev. Lett. **67**, 1882 (1991).

[5] G. Schütz and E. Domany, J Stat. Phys **72**, 277 (1993).

[6] B. Derrida, M. R. Evans, V. Hakim, and V. Pasquier, J Phys. A **26**, 1493 (1993).

[7] A. B. Kolomeisky, G. M. Schütz, E. B. Kolomeisky, and J. P. Straley, J. Phys. A **31**, 6911 (1998).

[8] V. Popkov and G. M. Schütz, Europhys. Lett **48**, 257 (1999).

[9] M. R. Evans, D. P. Foster, C. Godrèche, and D. Mukamel, J. Stat. Phys. **80**, 898 (1995).

[10] V. Popkov and I. Peschel, Phys. Rev. E **64**, 026126 (2001).

[11] E. Levine and R. Willmann, J. Phys. A **37**, 3333 (2004).

[12] A. Rakos and G. M. Schütz, J. Stat. Phys. p. to appear (2004).

[13] T. Antal and G. M. Schütz, Phys. Rev. E. **62**, 83 (2000).

[14] C. Bahadoran: Hydrodynamics of asymmetric particle systems with open boundaries, in preparation.

[15] G. M. Schütz, J. Phys. A **36**, R339 (2003).

[16] V. Popkov, J. Phys. A **37**, 1545 (2004).

[17] P. F. Arndt, T. Heinzel, and V. Rittenberg, J. Phys. A **31**, 831 (1998).

[18] V. Popkov and G. M. Schütz, J Stat. Phys. **112**, 523 (2003).

[19] J. Fritz and B. Tóth, Comm. Math. Phys. **249**, 1 (2004).

[20] D. Serre, *Systems of conservation laws, Vol.2* (Cambridge University Press, 2000).

[21] V. Popkov and M. Salerno, Phys. Rev. E **69**, 046103 (2004).

[22] C. Godrèche, J. M. Luck, M. R. Evans, D. Mukamel, S. Sandow, and E. R. Speer, J. Phys. A **28**, 6 (1995).

[23] R. Lahiri, M. Barma, and S. Ramaswamy, Phys. Rev. E **61**, 1648 (2000).

[24] D. Das, A. Basu, M. Barma, and S. Ramaswamy, Phys. Rev. E **64**, 021402 (2001).

[25] B. Tóth and B. Valkó, J Stat. Phys. **112**, 497 (2003).

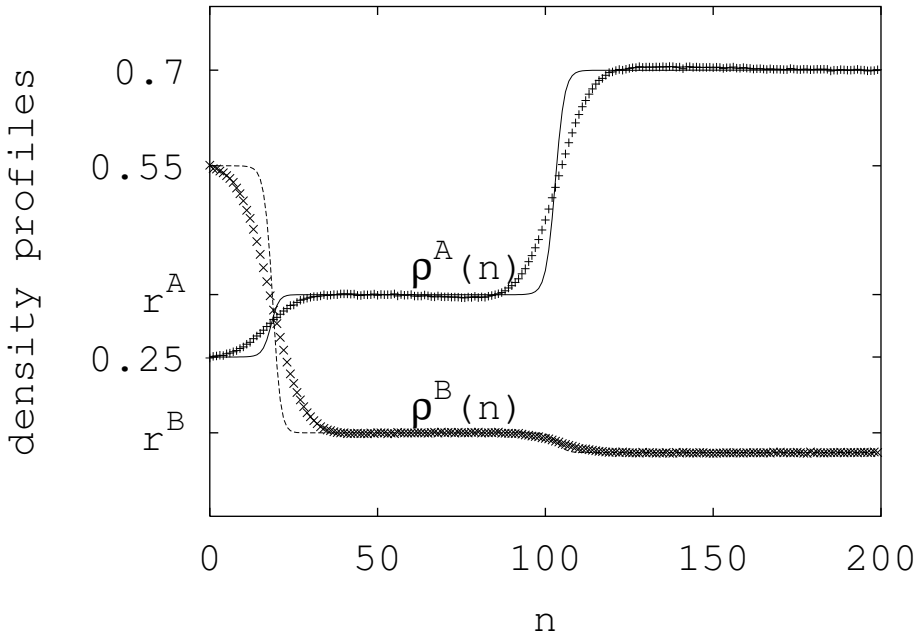

Figure 1: Domain wall reflection from the left boundary, as given by Monte Carlo simulations. Particles were initially distributed randomly without correlations with constant densities $\rho^A = 0.7, \rho^B = 0.1$, fitting the right boundary. The average profiles after 300 Monte Carlo steps are shown, and compared with the hydrodynamic limit (6) evolution (continuous curves). Averaging over $5{*}10^5$ histories is made. The smoothing of the Monte-Carlo density profile is due to fluctuations in the shock position which is scaled out in the hydrodynamic description.

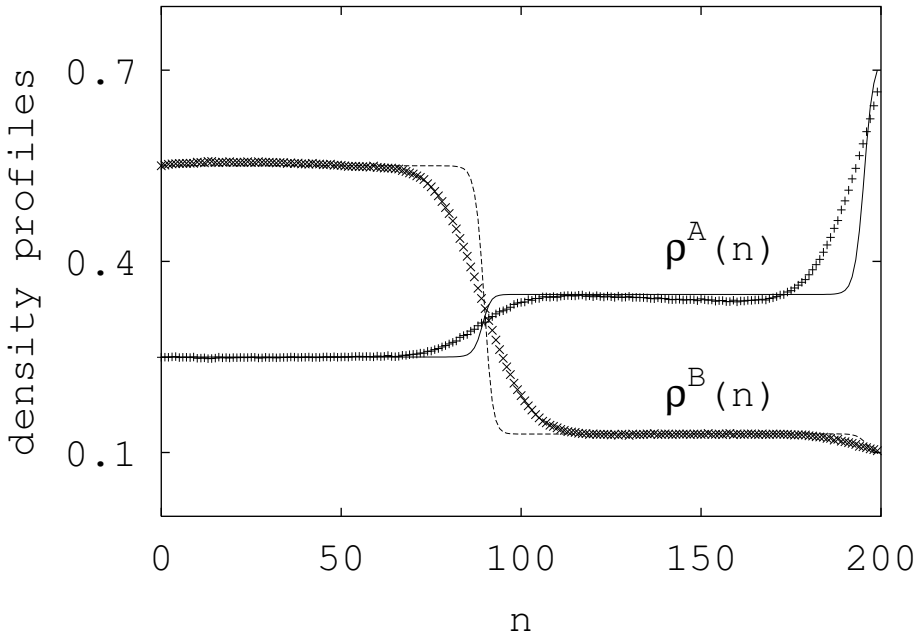

Figure 2: Domain wall reflection from the right boundary. Particles were initially distributed randomly without correlations with constant densities $\rho^A = 0.25, \rho^B = 0.55$ fitting the left boundary density. Average density profiles after $t = 300$ MCS steps are shown. The boundary densities are as on Fig. 1. Lines show the hydrodynamic evolution (6) for the two particle species. The smoothing of the Monte-Carlo density profile is due to fluctuations in the shock position which is scaled out in the hydrodynamic description.

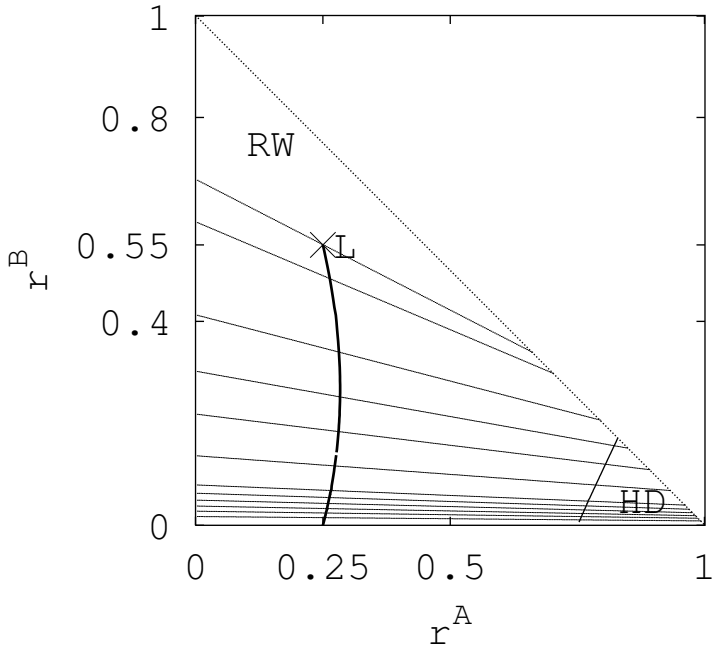

Figure 3: Left reflection map for the left boundary densities $0.25, 0.55$ of A and B particles respectively. The crossmark labelled L marks the point of the left boundary density. The curve containing this point L is a location of all possible densities r^A, r^B of the reflected waves, except at the region HD. The straight lines show initial bulk densities with the same outcome of a reflection (point of intersection of the straight line with the curve). In the HD region the initial wave stays glued to the left boundary. In the RW region (the upper triangle) the reflection results in a rarefaction wave (scaling as (x/t) with time), converging to point L. The dotted line $r^A + r^B = 1$ shows the boundaries of the physical region.

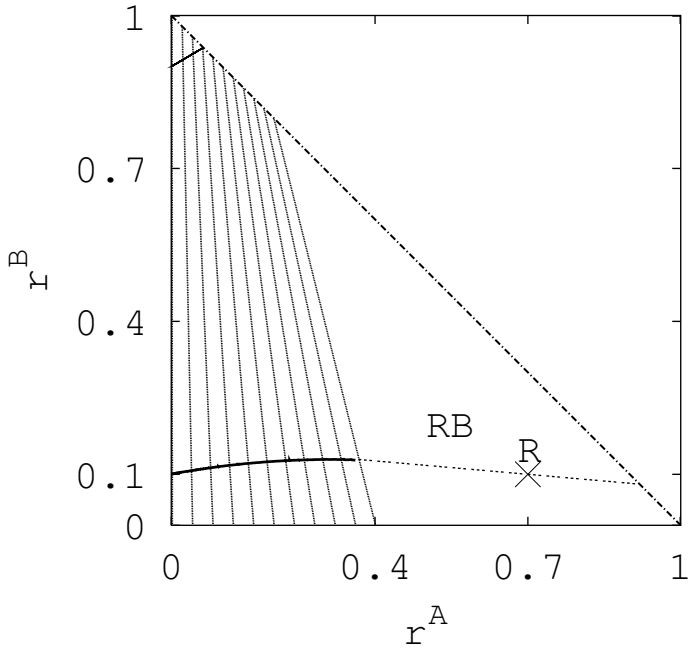

Figure 4: Right reflection map for the right boundary density $0.1, 0.7$ of A,B particles. The crossmark labelled R marks the point of the right boundary density. The thick curve is a location of all possible densities r^A, r^B of the reflected waves, except at the upper left triangle and in region RB. Straight lines show initial bulk densities with the same outcome of a reflection (point of intersection of the line with the thick curve). In the upper corner the initial wave stays glued to the right boundary. In the region RB an intermediate plateau appears, with the densities corresponding to the broken line passing through point R. The final result of this reflection is a wave matching the right boundary R. The dotted line $r^A + r^B = 1$ shows the boundaries of the physical region.

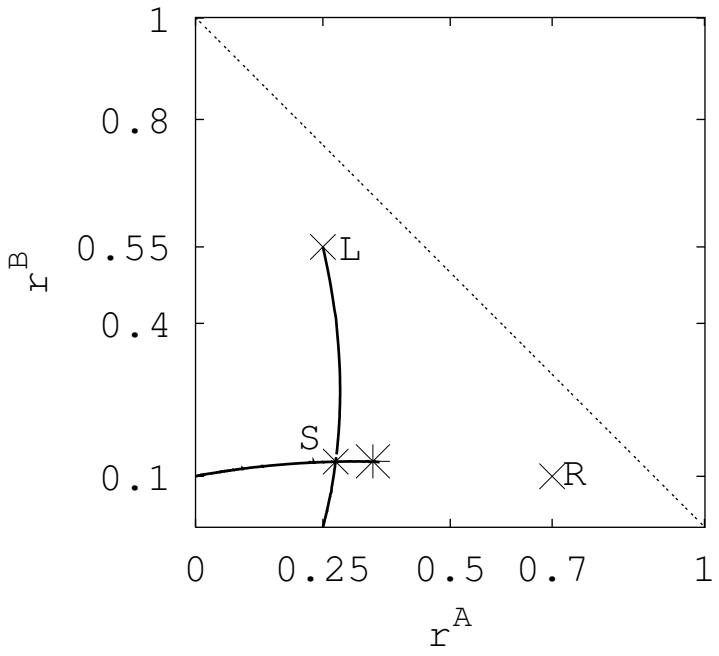

Figure 5: Curves of the right and left boundary reflection combined together. The intersection S, is the stationary state density achieved through the infinite number of reflections. The crossmarks labelled by R and L indicate the left and right boundary densities, and the cross at the intersection the stationary density obtained by Monte Carlo simulation of the system of 300 sites. The system was equilibrated for $= 4 * 10^5$ Monte Carlo Steps (MCS), after which the averaging over again $4 * 10^5$ MCS and 10 different histories was done. The big star to the righthand side of S marks the result of a single reflection for an initial profile fitting the left boundary density point L (from Monte Carlo calculations).

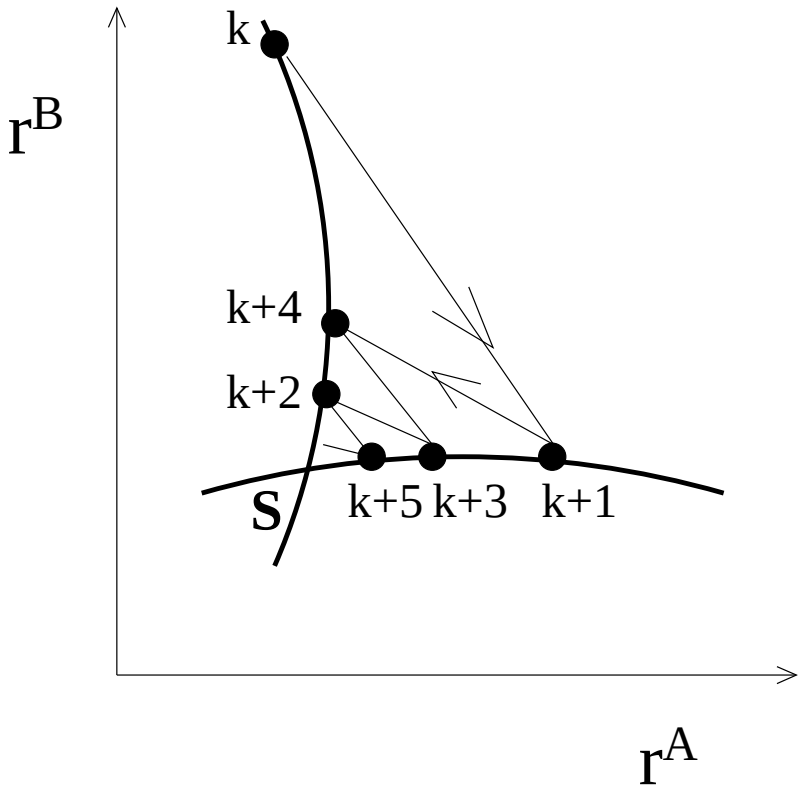

Figure 6: Approach to the stationary point S through an infinite sequence of reflections. The filled circles show the location of subsequent domain wall densities r^A, r^B. The circles $k, k+2, k+4$ correspond to the result of the left reflection, while the other circles correspond to the right reflection.

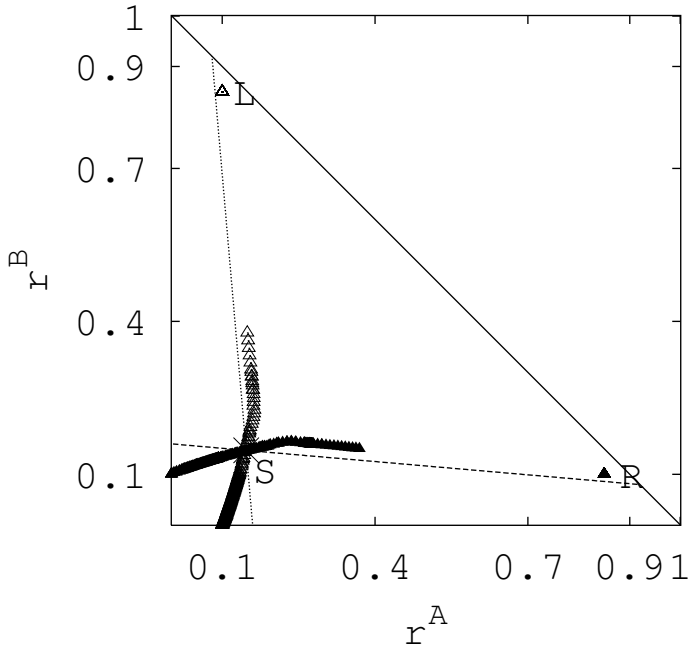

Figure 7: Curves of the right (filled triangles) and left (empty triangles) boundary reflection for the symmetric setting (24), as given by numerical integration of the hydrodynamic equations (6). Triangles labelled R and L indicate left and right boundary densities, and the point S the stationary density, achieved through an infinite series of reflections. The cross at the intersection point S marks the stationary density obtained by Monte Carlo simulation of the system of 300 sites. The broken and dotted lines intersecting at S show characteristic curves at the point S (see (21),(22)).